Journal of Science and Technology in Civil Engineering, HUCE, 2024, 18 (2): 45–55

AN EXPERIMENTAL AND NUMERICAL STUDY ON THE INNOVATIVE METALLIC BOX-SECTION DAMPER FOR IMPROVING THE BEHAVIOR OF CBF SYSTEMS

Chung Nguyen Van[a,*], Ali Ghamari[b]

[a]*Faculty of Civil Engineering, Ho Chi Minh City University of Technology and Education, 1 Vo Van Ngan Street, Thu Duc City, Ho Chi Minh, Vietnam*
[b]*Department of Civil Eng, Ilam branch, Islamic Azad University, Ilam, Iran*

Article history:
Received 04/03/2024, Revised 19/04/2024, Accepted 11/06/2024

Abstract

The susceptibility of the diagonal member of the Concentrically Braced Frames (CBFs) to buckling reduces the energy-dissipating capacity of the CBFs. Despite of high ultimate strength and stiffness of the CBFs as considerable advantages, its shortcoming (low dissipating energy capacity) is accounted as an important dilemma for this system. Although using metallic energy dampers, the seismic behavior of CBFs is enhanced, they impose more cost to structure and more constructional complicity. To address the issue, in this study, an innovative damper with a shear mechanism constructed as a box section was considered experimentally and numerically as well as parametrically. Results revealed that the proposed damper pertains to a suitable performance with stable hysteresis curves without degradation in stiffness, strength, and dissipating energy. The results also indicated that the overstrength of the damper reaches more than 1.5 (recommended by AISC). Moreover, a limitation as of $\rho > 0.55$, $\psi > 10$, and $67 < \lambda_w < 113$ was recommended to design the damper. Correspondingly, the required equations to design the damper were presented and were in good agreement with FE results.

Keywords: shear damper; box section; CBF; overstrength; stiffness; ultimate strength.

https://doi.org/10.31814/stce.huce2024-18(2)-04

1. Introduction

Comparing the conventional steel structures indicates that the concentrically braced frame systems (CBFs) have the greatest lateral strength and stiffness. However, it suffered from low ductility due to the buckling of diagonal members under compression loads. Accordingly, it leads the performance of the CBFs to a decrease in stiffness and energy absorption capabilities [1, 2]. Previous research has reported numerous strategies to solve this shortcoming, including designing appropriate demand-to-capacity ratios [3], utilizing specific configurations [4], and incorporating energy dissipation systems [5]. Utilizing energy dissipation systems is known as most effective in improving ductility and reducing seismic demand on structures among the mentioned strategies [6, 7].

Recently, researchers have confirmed the increasing interest in using metallic-hysteretic dampers to improve the behavior of the CBFs. Some of the popular dampers are: TADAS [8, 9], ADAS [10], shear dampers [4, 11], slit damper [12], and buckling restrained braces (BRBs) [13, 14]. These devices function within an eccentrically braced frame (EBF) system, converting the failure mechanism of CBFs from buckling to yielding specific elements. This mechanism change ends up increasing energy dissipation capacity. In line with the EBF systems, Pourbaba et al. [15] used a Zipper Braced Frame (ZBF) system to enhance the behavior of the CBFs. An experimental study using ductile gusset plates, called Centrically Fused Braced Frame (CFBF), proposed a strategy to enhance the seismic

*Corresponding author. *E-mail address:* chungnv@hcmute.edu.vn (Van, C. N.)

performance of CBFs. To ensure suitable seismic efficiency [16], economical aspects [4], easy fabrication [1, 2, 6], and capability to use for rehabilitation, Seki et al. [17] developed EBF systems utilizing a vertical shear link, V-EBF, between chevron brace and the floor beam. However, the main shortcoming of the V-EBF systems in comparison to conventional EBFs was lower elastic stiffness and higher construction cost [1]. In addition, these systems impose significant shear and moment actions on elements outside of the link due to yielding and strain hardening in the metallic damper [2, 18, 19]. Consequently, the floor beam may undergo nonlinear behavior during severe earthquakes, making it challenging to replace damaged dampers and floor beams after an earthquake. To compensate for this deficiency, Ghamari et al. [1, 6] developed an innovative metallic damper to improve the CBF systems. The main advantage of the proposed damper was preventing the bucking of the CBFs, which the damper yielded before other elements. Although the proposed system solves complicated issues regarding the replacement, it reduces the elastic stiffness and ultimate strength of the CBF system. To put forward the measure of shortcoming, in this paper, an innovative damper compound of box section is presented and investigated numerically and experimentally. The proposed damper possesses the advantages of the previous damper such as easy fabrication, capability of easy replacement, low cost to construct, and act as a ductile fuse. In addition to the mentioned advantages, since the box section is used for the damper, it is expected that it pertains greater moment of inertia in comparison to the shear plate or I-shaped damper. So, it stiffens and strength would be improved. So, the detail is addressed in the next sections.

2. Proposed damper

2.1. Detailing

In Fig. 1, a schematic view of the proposed damper is shown. As discovered in this figure, the damper consists of two types of elements main elements and secondary elements. Since the damper is added directly to the diagonal element braces, it can be installed easily. Accordingly, the detailing of the damper confirms that the proposed damper pertains to easier fabrication than other dampers. The main and secondary plates are welded together to create the damper. Correspondingly, the made damper can be welded or bolted to the CBFs' gusset plate to attach on the structure. The main elements provide the stiffness, strength, and ductility however the secondary elements produce the suitable performance of the main elements. The main and secondary elements, respectively, include the box

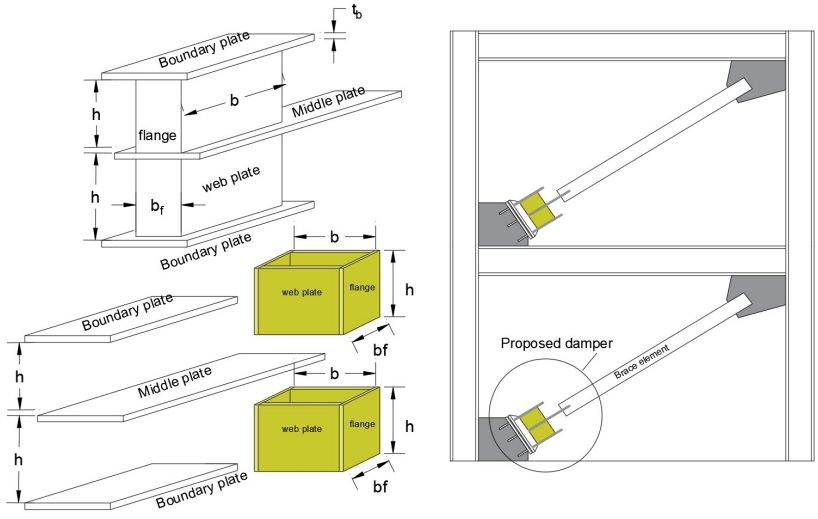

Figure 1. The general detailing of the proposed damper

section and boundary and middle plates. The main feature of the box section instead of the I-shaped section is that the box as a thin closed shape pertains to higher stiffness and strength in comparison to the I-shaped form while the same area section is used. Also, it has a higher out-of-plan strength against torsion and warping.

Therefore, it is expected that the nonlinear behavior of the system is limited to the main element, and other parts of the structure remain essentially elastic. Consequently, the damper can be easily replaced after a severe earthquake.

2.2. Design of the damper

According to the AISC 341-16, the shear strength of a box section when $\lambda_w \leq 1.10\sqrt{\frac{K_v E}{F_y}}$ is determined based on the Eq. (1), where λ_w is the web slenderness and is calculated as the ratio of web length divided by the web plate thickness. In this equation, the shear capacity is determined based on the shear strength of the web plate that the plate parallel to the applied loading is measured as the web plate. Also, the E and F_y are the modulus of elasticity and yielding stress, and the confession K_v is measured equal to 5.34.

$$V_p = 0.6F_{yw}bt_w \tag{1}$$

For a shear link, based on the AISC 341-16, the nominal shear strength, V_n, equals to plastic shear strength, V_P. Meanwhile, to impose the shear mechanism over the proposed damper, the box section must be satisfied the following relation.

$$\rho = \frac{V_p h}{M_p} \leq 1.6 \tag{2}$$

where h is the height of the box element. Correspondingly, M_p is the plastic moment of the box section that is calculated based on Eq. (3).

$$M_p = \frac{1}{2}\left[\frac{t_w b^2}{4} + b_f t_f \left(b + t_f\right)\right] \tag{3}$$

Although the effect of the flange plate on the shear strength of the box sections as well as the I-shaped section is ignored in AISC, in this paper, the flange plate effect on the damper capacity is considered. Subsequently, Eq. (4) is recommended to determine the shear strength of the box-section damper. Consequently, it is assumed that the shear strength of the damper, V_u, comprises of the web plate strength, V_p, and the flange plate strength, V_f. Also, coefficient 2 in this equation represents the two box sections used for constructing the damper.

$$V_u = 2\left(V_p + V_f\right) \tag{4}$$

Some researchers [20, 21] suggested accounting for the flange's effect in defining the shear capacity of the link that is considered in this paper. Accordingly, the V_f (shear capacity of the flange plates) is calculated using Eq. (4).

$$V_f = \frac{b_f t_f^2}{h} F_{yf} \tag{5}$$

where F_{yf} is the yielding stress of the flange plate. Other parameters have been introduced before.

To ensure the ductile behavior of the damper, elements outside of the damper are designed for forces presented in Eq. (6).

$$\begin{aligned} V_{design} &= 1.25 R_y V_u \\ V_{design} &= \Omega V_u \end{aligned} \tag{6}$$

where Ω is the over-strength that is considered in the next sections.

3. Experimental study

3.1. Test setup and material

To examine the proposed damper behavior, a specimen was tested under cyclic loading. Fig. 2 illustrates the specimen specification, prepared before and after the test. The plates with a thickness of 2 mm and a height of 110 mm were used to construct the box section. These properties were designed according to the universal acuter capacity and also to impose the shear mechanism on the box section. Also, plates with a thickness of 20mm were used for secondary elements. The Iranian steel called ST37 steel was used for all components of the dampers and its yielding stress and ultimate stress were 235 MPa, and 370 MPa, respectively. The specimen was tested under cyclic loading as $\mp\Delta y$, $\mp 2\Delta y$, etc where Δy displacement corresponds to yielding. Each cycle was repeated three times.

(a) Set up (b) The prepared specimen (c) The specimen after testing

Figure 2. Specimen specifications before and after cyclic loading test

3.2. Hysteresis curve results

At the first stage of applied cycle loading, the warping was visible over the web plates. Accordingly, at the displacement of 3 mm along with the diagonal of the web plate, the yielding was exposed. Consequently, by continuing the cyclic loading, tearing was shown noticeably on the flanges at the displacement of 12 mm (rotation of 10.9%). Therefore, the test was stopped. Fig. 3 illustrates the hysteresis curve of the proposed damper that is compared with the numerical simulation. The stable hysteresis curve without degradation in stiffness, strength, and dissipating energy up to rotation of 10.9% is revealed in the hysteresis curve. Also, only the box section was yielded, and no yielding occurred over the middle and boundary plates.

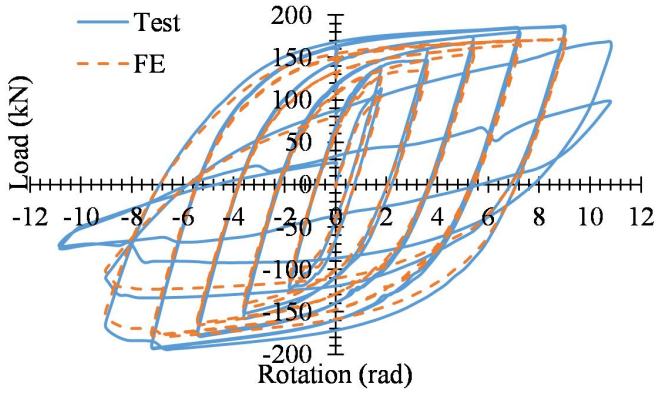

Figure 3. The experiment test results

3.3. Structural parameters

The ultimate strength of the damper was obtained under pull and push loading respectively equals 186.67 kN and 194.40 kN, which leads to a difference of around 4%. It is confirming the damper has a symmetrical behavior so, in the numerical study, the damper is evaluated under monotonic loading. The ductility of the damper was obtained 6, which is considerable. The damper started to yield at the load of +89 kN and −93.72 kN. These forces are accounted as the strength corresponding to the first plastic hinge in the damper. So, the overstrength, Ω, of the damper was obtained by 2.01. The Ω calculated for the damper is greater than 1.5 recommended by AISC for shear links. Therefore, it is required to complete a parametrical study to investigate the effect of variables on the Ω of the damper that is done in the numerical study.

4. Numerical study and discussion

4.1. Finite element simulating and verification of FE results

To investigate the behavior of the damper, a numerical study was carried out using the Finite Element (FE) method utilizing ANSYS software. For simulating the FE models, all parts of the models were modeled using SHELL 181. This element can consider the large deformation, yielding, bucking, and post-buckling.

For simulating the FE models, both materials and geometric nonlinearities were considered. In so doing, for accounting the material's nonlinearity effect, the stress-strain curve of the material was introduced to the software. Also, for geometric nonlinearity, an imperfection was applied to the models. To consider the initial geometrical imperfection, an eigenvalue buckling analysis was first performed, and then the obtained deformed shaped model with a coefficient of 1/1000 was updated to consider the imperfection. Comparing the results in Fig. 3 indicates a good agreement between FE results and test results.

4.2. Boundary condition and materials

The proposed damper was simulated with the same boundary condition as the experimental test. Accordingly, one end of the damper was restrained for displacement and rotation in all directions, and loading was applied to the damper at the other end of the damper. Since, according to AISC, the allowed rotation for shear links is 0.08 rad, the applied load to the FE models continued to reach the rotation of 0.08 rad. Also, the same material properties as the experimental test were used for FE models.

4.3. Details of parametrical models

A parametrical study was carried out to study the behavior of the proposed damper. In so doing, 28 FE models were designed and analyzed. So, some variables such as h, b_f, and b were considered. The same cross-section was selected for all models to have a fair comparison. So, the models including h = 50, 100, 150, with different b = 200, 280, 320, and 340 mm and different b_f = 160, 80, 40, and 20 mm were analyzed. For each model, a name was designed that contains five parts. The first part for all models, B, represents the box-section damper. The second stands for web plate length, b. Also, the third and fourth parts report the flange plate length, b_f, and flange plate thickness, t_f, respectively. Also, the last number represents the height, h, of the damper. For all models, the parameters A_w (section area) and t_w were kept constant at 2160 mm^2 and 3 mm, respectively. This gives a fair comparison between the FE models. The variables considered for the parametric study are the coefficients ρ and ψ. The parameter ψ is defined as $\psi = \dfrac{V_p}{V_f}$. The models were designed in such a way that the A_w kept constant. So, first, by keeping the A_w, the length of the flange plate, b_f, was reduced, and the b was increased. In the second plan, the b_f was reduced but its t_f was increased. Changing the parameters, b_f, t_f, and b in a constant ratio although keeping the A_w, they change the ρ, ψ, λ_w, and λ_f. The λ_w, and λ_f are the slenderness of the web plate and flange plate that are determined as $\lambda_w = \dfrac{b}{t_w}$ and $\lambda_f = \dfrac{b_f}{t_f}$, respectively. Also, the h was changed from 50 mm to 100, 150, and 200 mm to investigate the effect of the h that also changes the ρ and ψ.

5. Discussion and results on FE results

In Figs. 4 and 5, the yielding state of the analyzed damper is shown. As shown in this figure, yielding stress over the web is distributed. In models with long b, the yielding is formed along with the diagonal of the web plate. In the models with shorter heights, the yielding over the damper has a better distribution on the web plats. Also, for all models, the two plastic hinges are formed at the two ends of the flange plats. for the models with a long web plate and a low flange plate wide, the yielding over the web plate is not completely distributed. It is due to the fact that to complete the yielding of the web plate, the supportive role of the flange plate is required.

Fig. 6 discovers the effect of the height and flange on the stiffness of the damper. To do so, in the left column of the figure, the stiffness versus rotation for dampers with the same flange plate and different heights are plotted. Also, in the right column of the figure, the stiffness versus rotation for dampers with the same height and different flange are plotted.

As revealed in this figure, increasing the damper height reduces the stiffness. Moreover, up to rotation of 0.002 rad (beginning of the loading), no reduction in stiffness happened. After this rotation, stiffness reduction is seen but the reduction rate is different. Around a rotation of 0.007 rad, the stiffness of all dampers coincides together. It is confirmed that the stiffness in the nonlinear zone is not influenced by damper geometry. Moreover, the flange thickness affects the stiffness in the linear zone while the damper height is short. The damper with the same ρ does not have the same elastic stiffness. For instance, the models B-200-160-3-50 (ψ = 25) and B-200-80-6-50 (ψ = 12.5) have the same ρ = 0.23 but different elastic stiffness. Correspondingly, increasing the ψ improves the elastic stiffness.

To consider the effect of the damper geometry on the ultimate strength, V_u, V_s, and V/V_p, the results are listed in Table 1. The V_s is defined as yielding corresponds to the first yielding on the damper, and the V/V_p ratio is measured as the ratio of damper capacity to the yielding capacity of the damper.

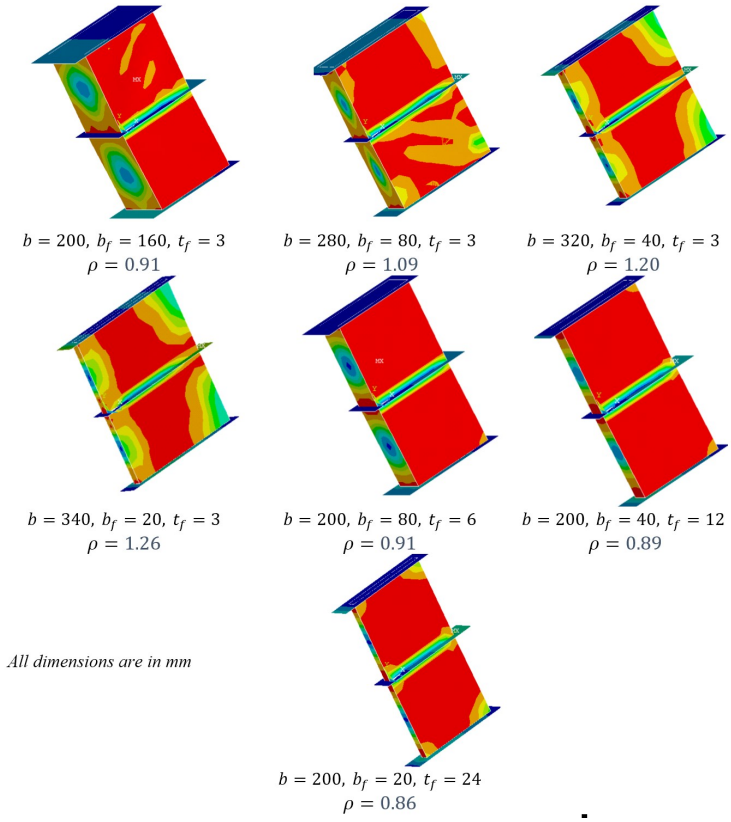

Figure 4. The yielding state of dampers with h = 200 mm

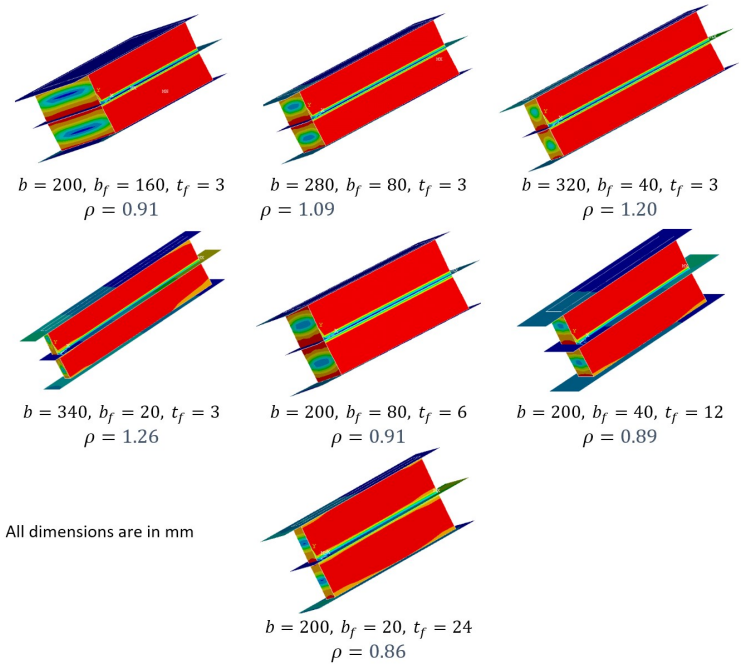

Figure 5. The yielding state of dampers with h = 50 mm

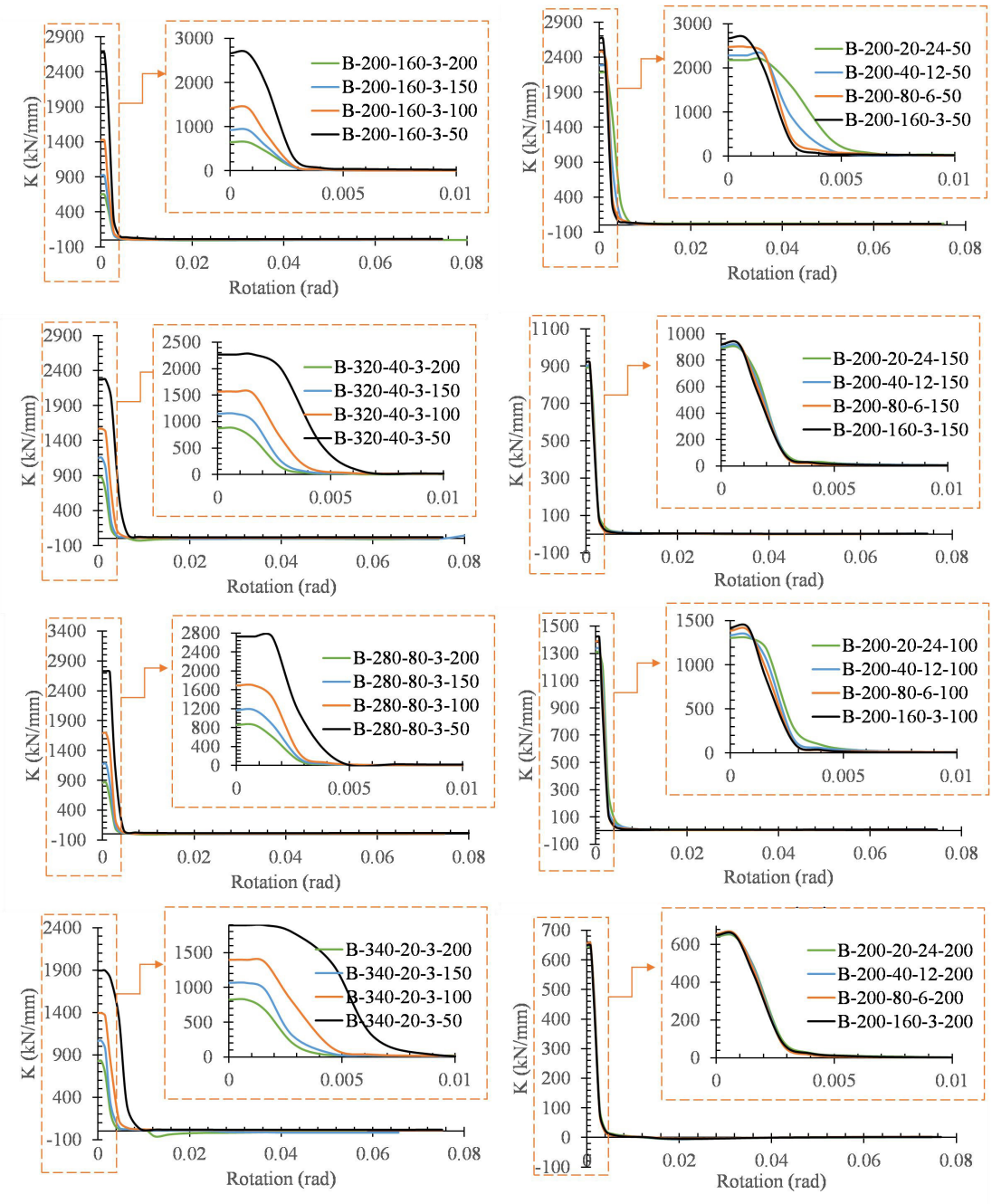

Figure 6. Stiffness versus rotation of the dampers with different height

Referring to the results, enhancing the damper height reduces the V_u, V_s, and V/V_p. The V_u reduction for damper with slenderness of $\lambda_w = 67, 93, 107$ and 113, respectively, is between 2% to 15%, 2% to 16%, 2% to 20%, and 2% to 21%. Also, for the damper with the mentioned slenderness, a reduction of 13%, 14%, 18%, and 20% is obtained. Nevertheless, by keeping the flange plate area properties and varying its slenderness, λ_f, from 53 to 13.3, 3.3, 0.8, the V_u is enhanced by a maximum 4%, 14%, and 38%.

Table 1. The ultimate strength of the dampers

Models	V_u (kN)	V/V_p	$\frac{damper\ h=1}{h=50}$		$\frac{damper=i}{\text{B-200-160-}i}$	
			V_u	V/V_p	V_u	V/V_p
B-200-160-3-50	412.90	1.17				
B-200-160-3-100	403.50	1.17	0.98	1.00		
B-200-160-3-150	376.81	1.09	0.91	0.93		
B-200-160-3-200	350.59	1.02	0.85	0.87		
B-280-80-3-50	550.69	1.12			1.33	0.96
B-280-80-3-100	539.99	1.12	0.98	1.00	1.34	0.96
B-280-80-3-150	490.51	1.02	0.89	0.91	1.30	0.93
B-280-80-3-200	462.78	0.96	0.84	0.86	1.32	0.94
B-320-40-3-50	618.38	1.10			1.50	0.94
B-320-40-3-100	608.17	1.10	0.98	1.00	1.51	0.94
B-320-40-3-150	540.00	0.98	0.87	0.89	1.43	0.90
B-320-40-3-200	496.88	0.90	0.80	0.82	1.42	0.89
B-340-20-3-50	650.70	1.09			1.58	0.93
B-340-20-3-100	639.15	1.09	0.98	1.00	1.58	0.93
B-340-20-3-150	559.61	0.96	0.86	0.88	1.49	0.87
B-340-20-3-200	513.74	0.88	0.79	0.80	1.47	0.86
B-200-80-6-50	429.00	1.19			1.04	1.02
B-200-80-6-100	410.57	1.19	0.96	1.00	1.02	1.02
B-200-80-6-150	375.80	1.09	0.88	0.92	1.00	1.00
B-200-80-6-200	352.71	1.02	0.82	0.86	1.01	1.01
B-200-40-12-50	470.84	1.23			1.14	1.05
B-200-40-12-100	423.42	1.23	0.90	1.00	1.05	1.05
B-200-40-12-150	380.86	1.10	0.81	0.90	1.01	1.01
B-200-40-12-200	356.33	1.03	0.76	0.84	1.02	1.02
B-200-20-24-50	571.17	1.34			1.38	1.15
B-200-20-24-100	462.45	1.34	0.81	1.00	1.15	1.15
B-200-20-24-150	395.77	1.15	0.69	0.86	1.05	1.05
B-200-20-24-200	366.00	1.06	0.64	0.79	1.04	1.04

6. Conclusions

In this paper, an innovative shear damper utilizing a box section directly attached to the diagonal member of CBF was proposed and considered experimentally and numerically. To examine the behavior of the damper and evaluate the effective variable on the damper behavior, a parametrical study was done. So, the main findings are summarized as follows:

- The suitable performance of the damper relying on hysteresis curve was confirmed using experimental test.

- The damper dissipated energy without degradation up to rotation of 10.9% that the rotation capacity is greater than the limitation of ASIC.

- Experimental as well as the numerical results revealed that the overstrength, Ω, of the proposed, is greater than AISC recommendation that is equals 1.5. Accordingly, Ω = 2.0 was suggested.

- Numerical study inidicated that increasing the height of the damper, h, reduces the elastic stiffness. Correspondingly, around a rotation of 0.007 rad, the stiffness of all dampers coincides together.

- By increasing the h from 50 mm to 200 mm, the elastic stiffness is reduced by 47% to 76%, 38% to 68%, 31% to 62%, and 26% to 56%, while the web plate is increased (from 200 mm to 280 mm, 320 mm, 340 mm, 340 mm, respectively) and flange plate is reduced (from 160 mm to 80 mm, 40 mm, 20 mm, respectively).

- Results indicated that the stiffness reduction for dampers with thick flange plates is lower than damper with large web plates.

- By keeping the flange plate area section and changing its slenderness, λ_f, from 53 to 13.3, 3.3, and 0.8, the ultimate strength is improved by a maximum of 4%, 14%, and 38%. Also, the V/V_p is enhanced by 2%, 5%, and 15%, respectively.

- By increasing the λ_w the ultimate strength of the models is reduced. Subsequently, designing models with $\lambda_w > 113$ is not suggested. Moreover, expect the model with $\lambda_w = 67$, the energy absorption of the models are increased while the $\rho < 0.9$. Accordingly, it is suggested to use models with $67 < \lambda_w < 113$.

Acknowledgments

The authors would like to thank Ho Chi Minh City University of Technology and Education, Vietnam for the support of time and facilities for this work.

References

[1] Thongchom, C., Bahrami, A., Ghamari, A., Benjeddou, O. (2022). Performance Improvement of Innovative Shear Damper Using Diagonal Stiffeners for Concentrically Braced Frame Systems. *Buildings*, 12 (11):1794.

[2] Ghamari, A., Kim, C., Jeong, S. (2022). Development of an innovative metallic damper for concentrically braced frame systems based on experimental and analytical studies. *The Structural Design of Tall and Special Buildings*, 31(8).

[3] Kumar, M. S., Senthilkumar, R., Sourabha, L. (2019). Seismic performance of special concentric steel braced frames. *Structures*, 20:166–175.

[4] Heidari, P. S., Jazany, R. A., Kayhani, H. (2012). An investigation on bracing configuration effects on behavior of concentrically braced steel frames. *World Applied Sciences Journal*, 17(9):1095–1108.

[5] Jaisee, S., Yue, F., Ooi, Y. H. (2021). A state-of-the-art review on passive friction dampers and their applications. *Engineering Structures*, 235:112022.

[6] Ghadami, A., Pourmoosavi, G., Talatahari, S., Azar, B. F. (2021). Overstrength factor of short low-yield-point steel shear links. *Thin-Walled Structures*, 161:107473.

[7] Ghadami, A., Pourmoosavi, G., Ghamari, A. (2021). Seismic design of elements outside of the short low-yield-point steel shear links. *Journal of Constructional Steel Research*, 178:106489.

[8] Tsai, K.-C., Chen, H.-W., Hong, C.-P., Su, Y.-F. (1993). Design of Steel Triangular Plate Energy Absorbers for Seismic-Resistant Construction. *Earthquake Spectra*, 9(3):505–528.

[9] Liyanage, U. D. D., Perera, T. N., Maneetes, H. (2020). Analysis of X-shaped and Double X-shaped Metallic Dampers on Multistorey Frames. *Journal of the University of Ruhuna*, 7(1):12–24.

[10] Xia, C., Hanson, R. D. (1992). Influence of ADAS element parameters on building seismic response. *Journal of Structural Engineering*, 118(7):1903–1918.

[11] Ghamari, A., Almasi, B., Kim, C.-h., Jeong, S.-H., Hong, K.-J. (2021). An Innovative Steel Damper with a Flexural and Shear–Flexural Mechanism to Enhance the CBF System Behavior: An Experimental and Numerical Study. *Applied Sciences*, 11(23):11454.

[12] Askariani, S. S., Garivani, S. (2020). Introducing and numerical study of a new brace-type slit damper. *Structures*, 27:702–717.

[13] Bai, J., Chen, H., Ma, G., Duan, L. (2022). Development of a four-tube-assembled buckling-restrained brace for convenient post-earthquake damage examination and replacement. *Journal of Building Engineering*, 50:104209.

[14] Saloma, Y. I., Hanafiah, N. O. (2017). Structural Behaviour of Steel Building with Diagonal and Chevron Braced CBF (Concentrically Braced Frames) by Pushover Analysis. *International Journal on Advanced Science, Engineering and Information Technology*, 7(2):716.

[15] Pourbaba, M., Karimia, M. R. G., Zareib, B., Azar, B. B. (2013). Behavior of Zipper Braced Frame (ZBF) compared with other Concentrically Braced Frame (CBF). *International Journal of Current Engineering and Technology*, 3(4):1202–1208.

[16] Menna, C., Felicioni, L., Negro, P., Lupíšek, A., Romano, E., Prota, A., Hájek, P. (2022). Review of methods for the combined assessment of seismic resilience and energy efficiency towards sustainable retrofitting of existing European buildings. *Sustainable Cities and Society*, 77:103556.

[17] Seki, M., Katsumata, H., Uchida, H., Takeda, T. (1988). Study on earthquake response of two-storied steel frame with Y-shaped braces. In *Proceedings 9th world conference on earthquake engineering, Tokyo-Kyoto, Japan*, volume 65.

[18] Ghadami, A., Pourmoosavi, G. (2022). Numerical investigation on the flange contribution in the shear strength of short LYP I-shaped links without intermediate stiffeners. *Structures*, 40:485–497.

[19] Baderloo, A. G., Pourmoosavi, G. (2023). The effect of heat-affected zone on the cyclic backbone curve of I-shaped LYP steel links. *Journal of the Brazilian Society of Mechanical Sciences and Engineering*, 45 (6).

[20] O'Reilly, G. J., Goggins, J. (2021). Experimental testing of a self-centring concentrically braced steel frame. *Engineering Structures*, 238:111521.

[21] Paronesso, M., Lignos, D. G. (2023). Influence of gravity connections and damper activation forces on the seismic behavior of steel CBF buildings with dissipative floor connectors. *Earthquake Engineering & Structural Dynamics*, 52(7):2135–2155.